Nuclear Instruments and Methods in Physics Research B 268 (2010) 1763–1767

Contents lists available at ScienceDirect

Nuclear Instruments and Methods in Physics Research B

journal homepage: www.elsevier.com/locate/nimb

# Effect of the Bethe surface description on the electronic excitations induced by energetic proton beams in liquid water and DNA

Isabel Abril [a,*], Cristian D. Denton [a], Pablo de Vera [a], Ioanna Kyriakou [b], Dimitris Emfietzoglou [b], Rafael Garcia-Molina [c]

[a] Departament de Física Aplicada, Universitat d'Alacant, Apartat 99, E-03080 Alacant, Spain
[b] Medical Physics Laboratory, University of Ioannina Medical School, Ioannina 451 10, Greece
[c] Departamento de Física – CIOyN, Universidad de Murcia, Apartado 4021, E-30080 Murcia, Spain

ARTICLE INFO

*Article history:*
Available online 26 February 2010

*Keywords:*
Energy-loss function
Dielectric formalism
Liquid water
DNA target
Energy loss
Proton beams
Electronic excitations

ABSTRACT

The irradiation of biological systems by energetic ion beams has multiple applications in medical physics and space radiation health, such as hadrontherapy for cancer treatment or protection of astronauts against space radiation. Therefore, for a better control and understanding of the effects of radiation damage in living tissues, it is necessary to advance an accurate description of the energy loss from the ion beam to the target. In the present work we use the dielectric formalism to calculate the probability for an energetic proton to produce electronic excitations in two targets of high biological interest, namely, liquid water and DNA. Also, the mean energy of the electronic excitations in these targets is found as a function of the incident proton energy. The electronic response of the target, characterized by its energy-loss function (ELF), is described by several models that fit the available experimental optical data (at zero momentum transfer), but use different approaches to obtain the Bethe surface, that is, to extend the ELF to any energy and momentum transferred.



## 1. Introduction

The study of the interaction of ionizing radiation (X-rays, electrons, positrons, protons or heavier ions) with living tissues has a paramount importance in cancer therapy, since the amount of energy deposited by the ionizing radiation to tumour cells will determine the outcome of the treatment [1,2]. Space radiation health is another area where research on proton and heavier ion effects on human tissues is important for the radiological protection of human crew in long-duration deep space missions [3].

The cure of tumours with hadrons (mainly protons and carbon ions) presents, with respect to the conventional X-ray and electron therapy, some advantages, from both the biological and physical point of view. The pattern of energy deposition by hadrons, called the Bragg peak, is characterized by most of the projectile energy deposited at the end of its range. In this way the damage to healthy cells, surrounding the malignant ones to be destroyed, can be strongly reduced [4–7].

The secondary electrons produced by ionizations induced in the living tissues by the projectile also contribute to the cellular damage. These electrons are able to travel and produce further ionizations in the DNA, eventually leading to the cellular death [8]. The lethal efficiency of each secondary electron depends on its energy [9,10], therefore it is very important to have information about the number and energy of the electrons generated by the projectile in the target. Even electrons with sub-ionizing energy were shown to produce lethal damage in DNA [9,11,12].

The aim of this paper is the calculation of the energy distribution of the electronic excitations produced by a proton when moving inside living tissues. Liquid water and DNA are the most relevant biological materials, hence we will focus on these materials as targets. Our approach to the problem will be through the well-known dielectric formalism [13] and a proper description of the target electronic response.

Several models have been proposed to describe the electronic response of the targets. Here we adopt the optical data methodology which overcomes the inherent shortcomings of Lindhard's electron–gas dielectric function to describe the excitation spectrum of non-free-electron-like materials with a wide band gap, such as liquid water and DNA. Different descriptions are examined for obtaining the complete excitation spectrum at arbitrary values of momentum transfer (Bethe surface). Furthermore we check their influence in the calculation of the energy distribution and the mean energy of the electronic excitations induced by a proton in liquid water and DNA.

The paper is structured as follows: the theoretical background is introduced in Section 2, while in Section 3 we present the details of

* Corresponding author. Tel.: +34 965909578; fax: +34 965909726.
*E-mail address:* ias@ua.es (I. Abril).

0168-583X/$ - see front matter © 2010 Elsevier B.V. All rights reserved.
doi:10.1016/j.nimb.2010.02.069

the models used to describe the energy-loss function of the target. Section 4 reviews the main results, and the conclusions are drawn in Section 5.

## 2. Theoretical model

When a swift projectile with mass $M_1$, atomic number $Z_1$, kinetic energy $T$ and charge $q$ moves inside a solid, it induces electronic excitations in the material, losing energy in the process. In the energy range to be discussed in the paper, this energy loss mechanism is the dominant one. These electronic excitations can correspond to excitations or ionizations of individual electrons or even excitations of collective modes in the target electron gas. The dielectric formalism [13] provides a way of studying the response of the electronic system of the target to the perturbation represented by the projectile. The key parameter of the problem is a correct description of the dielectric function of the material, $\varepsilon(k,\omega)$, which contains all the information about the electronic excitations that the material can sustain. Within this framework the probability per unit path length $P_q(T,E)$ that a projectile with charge state $q$ and energy $T$ produces in the target an excitation of energy $E=\hbar\omega$ irrespective of its momentum, $\hbar k$, is given by

$$P_q(T,E)=\frac{M_1e^2}{\pi\hbar^2T}\int_{k_{\min}}^{\infty}\frac{dk}{k}\rho_q^2(k)\mathrm{Im}\left[\frac{-1}{\varepsilon(k,\omega)}\right], \tag{1}$$

where $k_{\min}=\omega/\sqrt{2T/M_1}$, $e$ is the absolute value of the electron charge and $\rho_q(k)$ is the Fourier transform of the projectile charge density. Hence, the mean energy lost by the projectile per unit path length (the so called stopping power or stopping force) can be calculated integrating over all possible energy transfer $E$

$$\left.\frac{\langle\Delta T\rangle}{\Delta x}\right|_q=\int_0^{\infty}dE\,E\,P_q(T,E). \tag{2}$$

The mean energy of the electronic excitations $\langle E_q(T)\rangle$ induced by the projectile can be written as

$$\langle E_q(T)\rangle=\frac{\int_0^{\infty}dE\,E\,P_q(T,E)}{\int_0^{\infty}dE\,P_q(T,E)}. \tag{3}$$

The charge state $q$ of the projectile inside the target can vary through capture and loss processes and depends on its energy $T$. However, when charge equilibrium is reached, the probability $\phi_q(T)$ of finding the projectile in a charge state remains constant for each incident energy $T$. Here we obtain the values of $\phi_q(T)$ for hydrogen projectiles in liquid water or DNA using the parameterization provided by the CasP code [14], which uses Bragg's additivity rule for compound targets.

We average over all possible charge states ($q=0$ and 1 for H) in order to obtain the energy distribution, $P(T,E)$, and the mean energy, $\langle E(T)\rangle$, of the electronic excitations produced in the target as

$$P(T,E)=\sum_{q=0}^{1}\phi_q(T)P_q(T,E), \tag{4}$$

$$\langle E(T)\rangle=\frac{\int_0^{\infty}dE\,E\sum_{q=0}^{1}\phi_q(T)P_q(T,E)}{\int_0^{\infty}dE\sum_{q=0}^{1}\phi_q(T)P_q(T,E)}. \tag{5}$$

It is worth to notice that $\phi_0=0$ for $T$ greater than about 200 keV.

The calculation of the previous magnitudes requires the description of the projectile charge density through $\rho_q(k)$, and of the target excitation spectrum by means of its energy-loss function (ELF), $\mathrm{Im}[\frac{-1}{\varepsilon(k,\omega)}]$. The former is accounted for with the model proposed by Brandt and Kitagawa [15] because it is reliable and provides analytical expressions for $\rho_q(k)$. The latter will be discussed in the next section.

## 3. Description of the target ELF

Experimental information about the ELF at $k=0$ can be obtained for a number of materials, including liquid water and DNA, from the measurements of optical magnitudes. However, experimental information about the ELF at $k\neq0$ is limited. For this reason, it is necessary to model the evolution of the optical ELF with finite $k$ in order to calculate magnitudes such as $P$ and $\langle E\rangle$. Several models have been proposed to extend the optical ELF at finite $k$. Here we study the influence of the models in the calculation of $P$ and $\langle E\rangle$ for protons irradiating liquid water and DNA.

Fig. 1 depicts the ELF at $k=0$ of liquid water and DNA in a range of transfer energy $E$ corresponding to the excitation of outer-shell electrons of both materials. The symbols are experimental data for liquid water [16] and dry DNA [17]. The solid lines represent a fitting of the experiments [18,19] using a linear combination of Mermin-type ELFs [20]. We will extend these optical ELFs to finite values of $k$ using four different schemes, namely the extended-Drude model [21], the improved extended-Drude model [22,23], the Penn model [24], and the MELF–GOS model [25,26]. To unify further comparisons, a common treatment of the contribution of inner-shell excitations to the ELF will be done as explained in [25,26]; therefore, what follows only refers to the description of outer-shells excitations (unless otherwise started). A brief description of each model is made hereafter.

### 3.1. Extended-Drude model

In the extended-Drude model [21] the experimental ELF at $k=0$ is fitted with a linear combination of Drude-type ELFs:

$$\begin{aligned}\mathrm{Im}\left[\frac{-1}{\varepsilon(k,\omega)}\right]_{\text{outer}}&=\sum_i\frac{A_{\mathrm{D},i}}{\omega_i^2}\mathrm{Im}\left[\frac{-1}{\varepsilon_{\mathrm{D}}(\omega_i,\gamma_i;k,\omega)}\right]\Theta(\omega-\omega_{\mathrm{th},i})\\&=\sum_i\frac{A_{\mathrm{D},i}\gamma_i\omega}{\left\{[\omega_i(k)]^2-\omega^2\right\}^2+(\gamma_i\omega)^2}\Theta(\omega-\omega_{\mathrm{th},i}),\end{aligned} \tag{6}$$

where the subscript "D" stands for Drude; $A_{D,i}$, $\omega_i$, $\gamma_i$ and $\omega_{\mathrm{th},i}$ are the intensity, position, width and threshold, respectively, of the Drude-ELF peaks. $\Theta(\ldots)$ represents the Heaviside step function.

The extension at $k\neq0$ is done through a dispersion term for $\omega_i$ in the free-electron approximation:

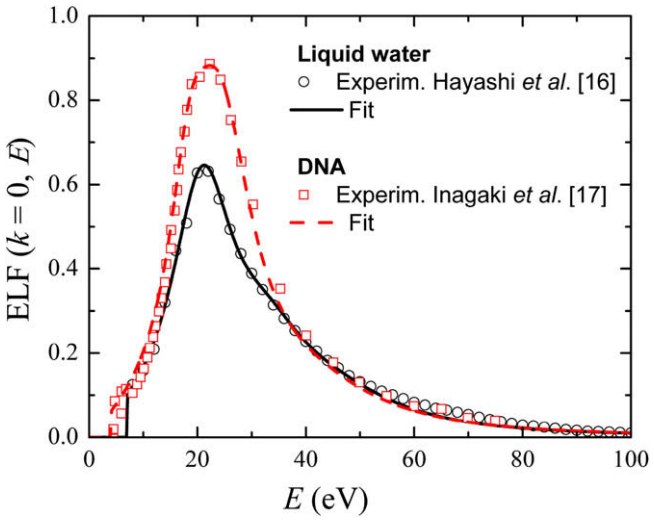


**Fig. 1.** ELF of liquid water and DNA in the optical limit ($k=0$) as a function of the transferred energy $E$. Symbols represent experimental data for liquid water [16] and dry DNA [17], while the curves correspond to a fitting using a linear combination of Drude-type ELFs.

$$\omega_i(k) = \omega_i + \frac{\hbar k^2}{2m}, \tag{7}$$

where $m$ is the electron mass. The above expression has the correct limiting behaviour at both the optical limit $k \to 0$ and over the Bethe ridge as $k \to \infty$.

### 3.2. Improved extended-Drude model

The model by Emfietzoglou and co-workers [22,23] is an improved version of the simple extended-Drude model described above. It accounts in a phenomenological way for the shifting and broadening of the Bethe ridge as observed experimentally [27] and predicted by local-field corrected electron–gas theory. The dispersion relations read:

$$\omega_i(k) = \omega_i + g(k)\,\frac{\hbar k^2}{2m}, \tag{8}$$

where $g(k) = 1 - \exp(-ck^d)$ and $\gamma_i(k) = \gamma_i + ak + bk^2$. For liquid water and DNA: $a$ = 10 eV, $b$ = 6 eV, $c$ = 1.2 and $d$ = 0.4 (assuming $k$ in a.u.). Note that the present value of the constant $c$ is somewhat smaller than previously reported [22] due to the slightly different Drude parameterization used in the two studies.

### 3.3. Penn model

Penn proposed a simpler scheme [24] where the sum over a finite number of Drude-type ELFs is replaced by an integration over Lindhard dielectric functions [13] of zero width. This integration yields the following evolution for finite $k$ [28]

$$\mathrm{Im}\left[\frac{-1}{\varepsilon(k,\omega)}\right]_{\mathrm{outer}} = \frac{\omega'(k)}{\omega}\,\mathrm{Im}\left[\frac{-1}{\varepsilon(k=0,\omega'(k))}\right], \tag{9}$$

where $\omega'(k) = \omega - \hbar k^2/2m$. If $\omega' \leqslant 0$, then $\mathrm{Im}[-1/\varepsilon(k,\omega)]$ is set to zero. In this way, the optical ELF is easily extended to $k \neq 0$ .

### 3.4. MELF–GOS model

In the MELF–GOS model [25,26] the ELF due to the outer electrons is modelled by a linear combination of Mermin-type ELFs [20]. One of the main advantages of this model is that an independent description for the dispersion of the optical peaks is not needed, unlike the previous models. The ELF can be automatically extended into all the range of $k$ through the analytical properties of the Mermin-type ELFs

$$\mathrm{Im}\left[\frac{-1}{\varepsilon(k,\omega)}\right]_{\mathrm{outer}} = \sum_i \frac{A_{D,i}}{\omega_i^2}\,\mathrm{Im}\left[\frac{-1}{\varepsilon_{\mathrm{M}}(\omega_i,\gamma_i;k,\omega)}\right]\Theta(\omega-\omega_{\mathrm{th},i}), \tag{10}$$

where $\varepsilon_{\mathrm{M}}$ is the Mermin dielectric function, which can be expressed in terms of the Lindhard dielectric function $\varepsilon_{\mathrm{L}}$ as

$$\varepsilon_{\mathrm{M}}(k,\omega) = 1 + \frac{(1+i\gamma/\omega)\,[\varepsilon_{\mathrm{L}}(k,\omega+i\gamma)-1]}{1+(i\gamma/\omega)\,[\varepsilon_{\mathrm{L}}(k,\omega+i\gamma)-1]/[\varepsilon_{\mathrm{L}}(k,0)-1]}. \tag{11}$$

The contribution to the ELF coming from the inner-shell electrons is taken into account in this model using generalized oscillator strengths (GOS) [29,30] of the target atomic constituents. For DNA ($C_{20}H_{27}N_7O_{13}P_2$), we consider as inner shell the K-shell of C, N, O and P, while for liquid water we only consider as inner-shell the K-shell of O. The resulting ELF is constrained to satisfy the $f$- and the KK-sum rules for every $k$ [31].

It is important to stress that the Mermin dielectric function coincides with the Drude dielectric function at $k$ = 0, hence the same fitting of the experimental ELF at $k$ = 0 is used for all the above models. As told previously, the extended-Drude, the improved extended-Drude, and the Penn models only take into account the ELF corresponding to the excitation of outer-shells, so for comparison purposes we will use the GOS approach for the inner-shells in these models.

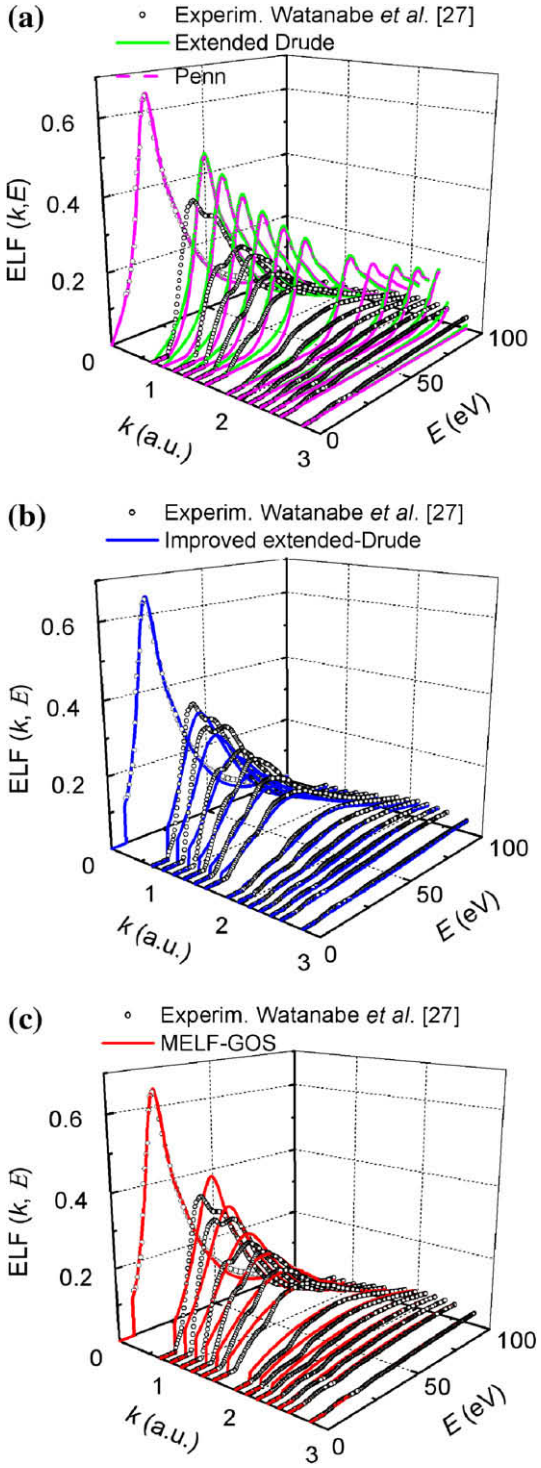


**Fig. 2.** ELF of liquid water at finite $k$. Symbols are experimental data [27], and lines represent the results of the different methods used to extend the ELF to finite values of $k$: (a) extended Drude (green solid lines) and Penn model (magenta dashed lines), (b) improved extended-Drude (blue lines) and (c) MELF-GOS (red solid lines). (For interpretation of the references to colour in this figure legend, the reader is referred to the web version of this article.)

In order to check the reliability of each model in describing the ELF at finite $k$ we have compared the calculated ELF with available experimental results. Using the IXS technique, Watanabe et al. [27] measured the ELF of liquid water at a few values of $k \neq 0$. In Fig. 2 we show the experimental values of the ELF of liquid water repre-

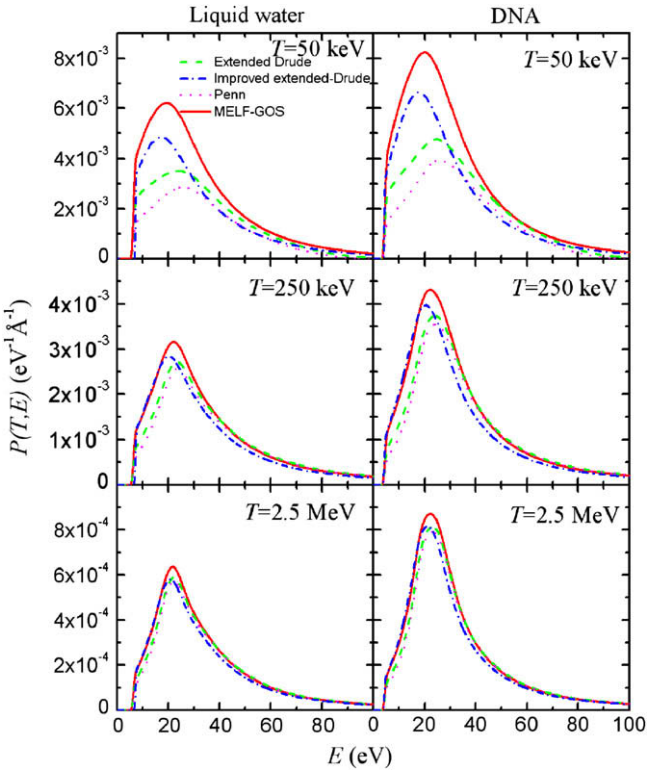


**Fig. 3.** Probability per unit path length $P$ that a H projectile induces electronic excitations of energy $E$ in liquid water and DNA. Results for projectile energies $T = 50$, 250 and 2500 keV are displayed. The lines represent the calculations obtained when modelling the ELF with the extended-Drude model (green dashed lines), the improved extended-Drude model model (blue dash-dotted lines), the Penn model (magenta dotted lines), and the MELF-GOS model (red solid lines). (For interpretation of the references to colour in this figure legend, the reader is referred to the web version of this article.)

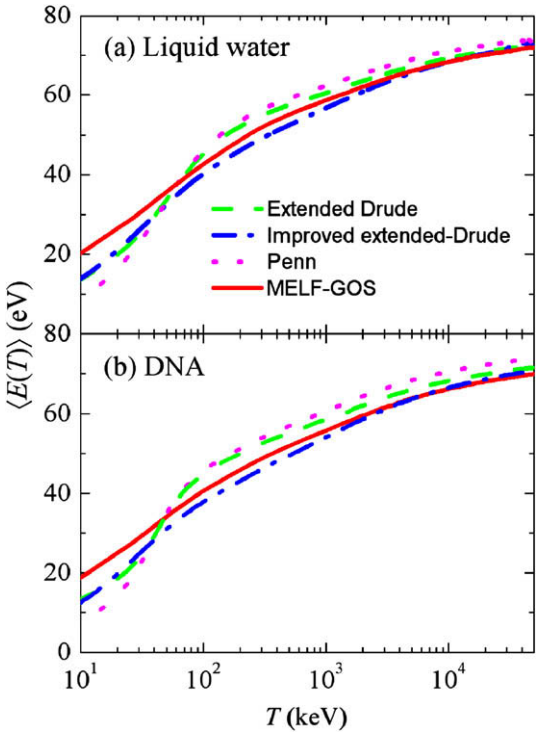


**Fig. 4.** Mean energy $\langle E(T)\rangle$ of the excitations induced by a hydrogen projectile in (a) liquid water and (b) DNA as a function of the projectile energy $T$. The lines represent the calculations obtained when modelling the ELF with the extended-Drude model (green dashed lines), the improved extended-Drude model (blue dash-dotted lines), the Penn model (magenta dotted lines), and the MELF–GOS model (red solid lines). (For interpretation of the references to colour in this figure legend, the reader is referred to the web version of this article.)

sented by symbols compared with the calculations of the ELF using the different models. Fig. 2(a) corresponds to the extended-Drude and the Penn models, Fig. 2(b) to the improved extended-Drude model and Fig. 2(c) shows the results of the MELF–GOS model. We observe that the first two models, producing almost the same results, disagree with the experimental ELF. On the other hand, both the the improved extended-Drude and the MELF–GOS models provide a much more realistic behaviour of the ELF at $k \neq 0$ .

## 4. Results

Fig. 3 depicts the calculated probability per unit path length $P(T,E)$, Eq. (4), for a proton beam (having incident energies $T = 50$ keV, 250 keV and 2.5 MeV) of producing an electronic excitation of energy $E$ in liquid water and DNA. We have included in the figure the calculations obtained by using the extended Drude (dashed lines), the improved extended-Drude (dash-dotted lines), the Penn (dotted lines), and the MELF–GOS (solid lines) models. We observe that, regardless of the chosen model, for any projectile energy $T$ there is a maximum of electronic excitations at transferred energies $E$ around 25 eV. Also we find that the probability $P$ decreases as the proton energy increases, indicating that a larger number of electronic excitations are produced when lower incident energies $T$ are used.

The values of $P$ predicted by all the models agree at large $T$, however there are sizeable differences at intermediate and small $T$. This is very important because this range of $T$ corresponds to the Bragg peak, where most of the projectile energy is deposited. This disagreement is caused by an incorrect description of the low $k$ electronic excitations in the extended-Drude and Penn models.

The mean energy $\langle E(T)\rangle$, Eq. (5), of the electronic excitations produced by a proton in liquid water and in DNA is depicted in Fig. 4. It is seen that $\langle E(T)\rangle$ increases with the proton energy $T$, being around 10–20 eV at $T = 10$ keV and around 70 eV for $T = 5 \times 10^4$ keV. As the number of electronic excitations, characterized by $P(T,E)$, decreases with $T$, and the mean energy of the excitation increases with $T$, hence a maximum in the stopping power, Eq. (2), is clearly expected. We have found that for liquid water and DNA this maximum appears around $T = 100$ keV [18,19].

The secondary electrons generated by the protons will have an energy $E_{sec} \cong \langle E\rangle - E_{bind}$, where $E_{bind}$ is a representative value characterizing the binding energy of the target electrons. For the case of liquid water $E_{bind}$ is of the order of 10 eV [10]. Therefore, the generated secondary electrons could be very effective in producing DNA strand breaks, due to the low threshold energy for radiation damage in biomolecules [32].

## 5. Conclusions

We have calculated the spectral distribution of the electronic excitations induced by a proton in liquid water and dry DNA. For this purpose we use the dielectric formalism and obtain the target energy-loss function, $\mathrm{Im}[-1/\varepsilon(\omega,k)]$, from optical data and four different models to describe its extension to arbitrary values of momentum-transfer $k$, namely the extended-Drude [21], the improved extended-Drude [22,23], the Penn [24], and the MELF–GOS [25,26] models. We find that, regardless of the proton energy, the probability distribution $P$, of the electronic excitations has a maximum around 25 eV. Besides, $P(E,T)$, which is related to the number of electronic excitations of a given energy $E$, decreases

with the proton energy $T$. On the other hand the mean energy $\langle E(T)\rangle$ of the electronic excitations increases monotonically with the proton energy $T$ ranging from ~10–20 eV at $T = 10$ keV to ~70 eV to $T = 5 \times 10^4$ keV. All the models examined agree in the calculation of $P(T,E)$ and $\langle E(T)\rangle$ at large values of the proton energy. At lower projectile energies important differences arise among the models. The improved extended-Drude and the MELF–GOS models, are the most reliable since they provide a more realistic description of the ELF of liquid water at finite transferred momentum, as compared with experiments. We therefore expect that they would also be more reliable for DNA, as also holds for other non-free-electron-like materials [33,34]. However, momentum-dependent EELS and/or IXSS measurements on DNA are desperately needed to validate model calculations for the energy loss of charged particles in these important biological materials.

## Acknowledgments

This work has been financially supported by the Spanish Ministerio de Ciencia e Innovación (Project Nos. FIS2006-13309-C02-01 and FIS2006-13309-C02-02) and the European Union FP7 ANTICARB (HEALTH-F2-2008-201587). CDD thanks the Spanish Ministerio de Ciencia e Innovación and Generalitat Valenciana for support under the Ramón y Cajal Program. PdV acknowledges the Universitat d'Alacant for a research grant.

## References

[1] H. Breuer, B.J. Smit, Proton Therapy and Radio-surgery, Springer, Berlin, 2000.
[2] E.B. Podgorsak, Radiation Physics for Medical Physicist, Springer, Berlin, 2006.
[3] M. Durante, F.A. Cucinotta, Nat. Rev. Cancer 8 (2008) 465.
[4] G. Kraft, Nucl. Instrum. Methods Phys. Res., Sect. A 454 (2000) 1.
[5] G. Kraft, Prog. Part. Nucl. Phys. 45 (2000) S473.
[6] O. Jäkel, Ion Beam Science: Solved and Unsolved Problems, in: P. Sigmund (Ed.), Matematisk-fysiske Meddelelser 52, Copenhagen, 2006, p. 37.
[7] H. Nikjoo, S. Uehara, D. Emfietzoglou, A. Brahme, New J. Phys. 10 (2008) 075006.
[8] Z. Cai, P. Coutier, J. Phys. Chem. B 109 (2005) 4796.
[9] B. Boudaïffa, P. Cloutier, D. Hunting, M.A. Huels, L. Sanche, Science 287 (2000) 1658.
[10] L. Sanche, Radiat. Prot. Dosim. 99 (2002) 57.
[11] J. Simons, Acc. Chem. Res. 39 (2006) 772.
[12] A.V. Solov'yov, E. Surdutovich, E. Scifoni, I. Mishustin, W. Greiner, Phys. Rev. E 79 (2009) 011909.
[13] J. Lindhard, K. Dan, Vidensk Selsk, Mat.-Fys. Medd. 28 (8) (1954).
[14] P. L. Grande, G. Schiwietz, CasP. Convolution approximation for swift Particles, version 3.1 (2005) available from http://www.hmi.de/people/schiwietz/casp.html.
[15] W. Brandt, M. Kitagawa, Phys. Rev. B 25 (1982) 5631.
[16] H. Hayashi, N. Watanabe, Y. Udagawa, C.-C. Kao, Proc. Natl Acad. Sci. USA 97 (2000) 6264.
[17] T. Inagaki, R.N. Hamm, E.T. Arakawa, L.R. Painter, J. Chem. Phys. 61 (1974) 4246.
[18] R. Garcia-Molina, I. Abril, C.D. Denton, S. Heredia-Avalos, I. Kyriakou, D. Emfietzoglou, Nucl. Instrum. Methods Phys. Res., Sect. B 267 (2009) 2647.
[19] I. Abril, R. Garcia-Molina, C. D. Denton, I. Kyriakou, D. Emfietzoglou, (2010), in press.
[20] N.D. Mermin, Phys. Rev. B 1 (1970) 2362.
[21] R.H. Ritchie, A. Howie, Phil. Mag. 36 (1977) 463.
[22] D. Emfietzoglou, F.A. Cucinotta, H. Nikjoo, Radiat. Res. 164 (2005) 202.
[23] D. Emfietzoglou, R. Garcia-Molina, I. Kyriakou, I. Abril, H. Nikjoo, Phys. Med. Biol. 54 (2009) 3451.
[24] D.R. Penn, Phys. Rev. B 35 (1987) 482.
[25] I. Abril, R. Garcia-Molina, C.D. Denton, F.J. Pérez-Pérez, N.R. Arista, Phys. Rev. A 58 (1998) 357.
[26] S. Heredia-Avalos, R. Garcia-Molina, J.M. Fernández-Varea, I. Abril, Phys. Rev. A 72 (2005) 052902.
[27] N. Watanabe, H. Hayashi, Y. Udagawa, Bull. Chem. Soc. Jpn 70 (1997) 719.
[28] Z.J. Ding, R. Shimizu, Scanning 18 (1996) 92.
[29] U. Fano, Annu. Rev. Nucl. Part. Sci. 13 (1963) 1.
[30] R.F. Egerton, Electron Energy-Loss Spectroscopy in the Electron Microscope, Plenum Press, New York, 1989.
[31] E. Shiles, T. Sasaki, M. Inokuti, D.Y. Smith, Phys. Rev. B 22 (1980) 1612.
[32] L. Sanche, Eur. Phys. J. D 35 (2005) 367.
[33] S. Heredia-Avalos, J.C. Moreno-Marin, I. Abril, R. Garcia-Molina, Nucl. Instrum. Methods Phys. Res., Sect. B 230 (2005) 118.
[34] R. Garcia-Molina, I. Abril, C.D. Denton, S. Heredia-Avalos, Nucl. Instrum. Methods Phys. Res., Sect. B 249 (2006) 6.